

Magnetic Excitons in Space-Charge Layers in GaAs

E. Batke^(a) and C. W. Tu

AT&T Bell Laboratories, Murray Hill, New Jersey 07974

(Received 25 June 1986)

We have studied the high-frequency conductivity of multilayer two-dimensional electron systems on GaAs in perpendicular magnetic fields with far-infrared transmission spectroscopy. In addition to cyclotron excitation, new resonances with energies close to the cyclotron frequency are observed. Their number and dependence on the magnetic field strength and charge density are consistent with those theoretically predicted for two-dimensional magnetic excitons.

PACS numbers: 71.45.Gm, 72.20.My, 73.40.Lq, 78.20.Ls

A magnetic field perpendicular to the plane of a quasi two-dimensional (2D) space-charge layer quantizes the free in-plane motion in discrete Landau levels. In a classical 2D system the elementary single-particle and collective intrasubband excitations are cyclotron resonance (CR) and magnetoplasmons, respectively. Both are associated with transitions between Landau levels but the latter involve a finite wave-vector transfer q .¹ The magnetoplasmon dispersion $\omega_{\text{mp}}(q)$ in the long-wavelength limit $X = \mathbf{q} \cdot \mathbf{k}_F l^2 \ll 1$ [\mathbf{k}_F is the Fermi wave vector; $l = (\hbar/eB)^{1/2}$ is the lowest cyclotron orbit] in random-phase approximation follows the relation¹

$$\omega_{\text{mp}}^2(q) = \omega_c^2 + \omega_p^2(q), \quad (1)$$

where $\omega_c = eB/m_c$ is the cyclotron frequency and $\omega_p(q)$ is the 2D plasmon dispersion for vanishing magnetic field.² In the short-wavelength limit $X \gg 1$ the magnetoplasmon frequencies are restricted to the vicinity of ω_c and its multiples:

$$\omega_{\text{mp}}(q) = n[\omega_c + F_n(X)], \quad n = 1, 2, \dots, \quad (2)$$

where $F_n(X)$ is a positive, monotonically decreasing, oscillatory function of X .¹ Electron-electron interaction affects the magnetoplasmon dispersion significantly in the short-wavelength limit.³⁻⁵ In addition, the electron-electron interaction establishes spin and coupled magnetoplasmon-spin modes and all these new dispersions are referred to as magnetic excitons.⁴ From experimental studies of the exciton dispersions in the short-

wavelength limit valuable information can be gained on the importance of many-body effects in 2D systems. In this Letter we report the first experimental evidence for magnetic excitons. They are observed in cyclotron excitation on modulation-doped $\text{Al}_x\text{Ga}_{1-x}\text{As}$ -GaAs multiple quantum wells (MQW).

We studied MQW grown by molecular-beam epitaxy with different mobilities μ , charge densities per well N_s , numbers of wells, and periodicities d . A representative set is listed in Table I. N_s and μ were determined by Shubnikov-de Haas and van der Pauw measurements, respectively. From the Shubnikov-de Haas experiments there is no evidence for the population of a second subband indicating that the Fermi energies are smaller than the subband separations.

We studied CR in far-infrared transmission on wedged samples at temperature 4.3 K in fixed perpendicular magnetic fields with a rapid-scan Fourier-transform spectrometer. We compare two transmission spectra $T(B)$ at zero and finite perpendicular magnetic field B to obtain the dimensionless normalized transmission $\Delta T/T$:

$$\frac{\Delta T}{T} = \frac{T(B=0) - T(B)}{T(B=0)}.$$

Figure 1 compares experimental and calculated (dotted lines) $\Delta T/T$ for samples 1 and 3 at different magnetic fields. The filled arrows mark CR positions. The calculation assumes perpendicularly incident, linearly polarized far-infrared radiation and a Drude-type three-

TABLE I. MQW with period $d = d_{\text{Ga}} + d_{\text{Al}} + 2d_{\text{S}}$. Here d_{Ga} , d_{Al} , and d_{S} correspond to the well width, the doped $\text{Al}_x\text{Ga}_{1-x}\text{As}$ layer, and the undoped $\text{Al}_x\text{Ga}_{1-x}\text{As}$ (spacer) layer, respectively. N_s and μ are the surface charge density and mobility for one well, respectively.

Sample	d_{Ga} (Å)	d_{Al} (Å)	d_{S} (Å)	Number of wells	N_s (10^{11} cm^{-2})	μ ($10^3 \text{ cm}^2/\text{V}\cdot\text{s}$)
1	200	75	200	30	1.9 ± 0.1	120
2	277	271	217	15	3.0 ± 0.2	140
3	200	150	200	30	3.9 ± 0.2	260
4	139	64	170	50	5.2 ± 0.2	75

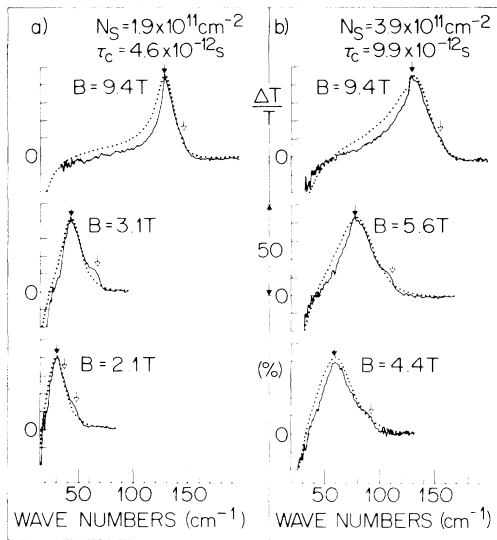


FIG. 1. Experimental $\Delta T/T$ vs energy for (a) sample 1 and (b) sample 3 for different magnetic fields B . CR (HER) positions are marked by solid arrows (open arrows). The dotted curves represent calculated $\Delta T/T$ on the assumption of a Drude-type well conductivity. The calculated CR amplitudes are adjusted to the experimental ones by scaling.

dimensional well conductivity

$$\sigma_{\pm} = \frac{N_s e^2 \tau_c}{d_{\text{Ga}} m_c} \frac{1}{1 + i(\omega \pm \omega_c) \tau_c},$$

with τ_c replaced by τ_{dc} , obtained from the mobility. The MQW CR line shapes are broad and asymmetric because of the multilayered nature of the structure and the high total charge density. The full widths at half maxima (FWHM) are ruled by the high total charge density [$N_s \times$ (number of wells)], while μ is of minor importance. For our samples 1 and 3 the theory predicts complete signal saturation, i.e., $\Delta T/T = 50\%$, at $\omega = \omega_c$. The experimental CR amplitudes do not exceed $(44 \pm 1)\%$ for either sample. We attribute this discrepancy to shifts in excitation strength and/or to CR-inactive regions in the macroscopic sample area and have adjusted the calculated CR amplitudes to the experimental ones by scaling (Fig. 1). Even more importantly, the calculated $\Delta T/T$ gives no explanation for satellite resonances in the experimental spectra (marked in Fig. 1 with open arrows).

Three new resonances, two with energies larger than ω_c and one with energy lower than ω_c , are found on low-mobility and low-density MQW. The magnitude of the shift with respect to ω_c is smaller for the resonance with $\omega < \omega_c$ compared to the resonances with $\omega > \omega_c$. Their observability depends on the mobility and total charge density of the MQW. In high-density, high-mobility MQW as listed in Table I the resonances which stay close to ω_c can be masked by the CR background absorption. Therefore the resonance with $\omega < \omega_c$ could

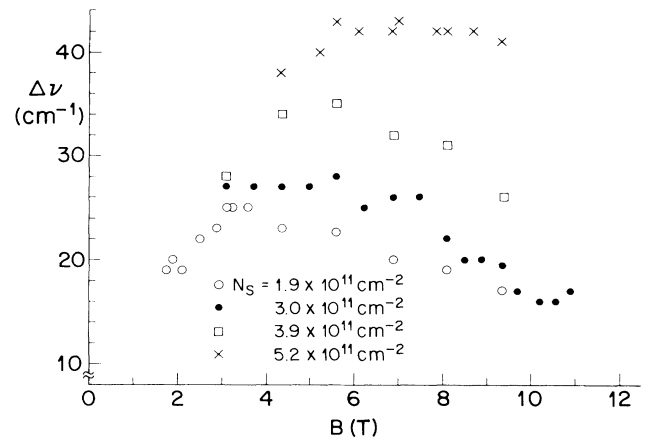


FIG. 2. Shifts $\Delta\nu = \Delta\omega/2\pi c = \nu_{\text{HER}} - \nu_c$ in wave numbers for all MQW listed in Table I vs magnetic field strength. The uncertainty in picking the peak positions for all N_s is less than 3 cm^{-1} .

not be identified on samples 1 and 3, but is seen weakly in sample 2. Two satellite resonances with $\omega > \omega_c$ are observed for sample 1 at low magnetic fields [Fig. 1(a), $B = 2.1 \text{ T}$], whereas only one resonance is clearly resolved for sample 3. The most prominent satellite resonance, to which we will refer as high-energy resonance (HER) with largest positive shift $\Delta\omega = \omega - \omega_c$, however, is observed in all MQW. In Fig. 2 the shift ($\omega_{\text{HER}} - \omega_c$) is shown for all MQW of Table I versus magnetic field strength. The shift increases with increasing N_s and is largest for a certain magnetic field $B_c(N_s)$. From B_c the shift decreases with increasing and decreasing magnetic field strength. This means that the satellite resonance position approaches ω_c for high and low magnetic fields.

The FWHM of the satellite resonances do not depend sensitively on N_s and μ which is in contrast to the observed N_s broadening of the CR line shape. The FWHM of the resonances with $\omega > \omega_c$ for all samples cover a range $9 \pm 3 \text{ cm}^{-1}$ while the FWHM of the resonance with $\omega < \omega_c$ can be up to a factor of 2 smaller. The absorption strength is about 3% and is estimated by comparison of the integral over the satellite resonances divided by the number of wells to the calculated integral over the CR of a single layer.

Helicons can be excluded as a possible explanation for our satellite resonances since they are restricted to a frequency regime $\omega < \omega_c$ and show a linear frequency-magnetic-field dependence.⁶ The satellite resonances have no analogy to anomalies reported for CR in single-interface 2D systems. Harmonic CR⁷ can be ruled out, since the new resonance positions do not scale with multiples of ω_c . Splittings of the CR and line-shape anomalies of single-interface heterostructures on GaAs correlated with N_s have previously been reported by Schlesinger *et al.*⁸ We find qualitatively similar effects for MQW with low total charge density, i.e., few

wells and low N_s ($N_s \leq 3 \times 10^{11} \text{ cm}^{-2}$). However, there is no obvious correlation between those CR anomalies and our satellite resonances. We also can exclude effects arising from the coupling of CR to intersubband resonances, which depends strongly on the tilt angle θ of the magnetic field B with respect to the interface normal. In tilted-field configuration CR–intersubband-resonance coupling can result in a splitting of the CR line shape if $\hbar\omega_c$ equals the subband resonance energy E_{01} .⁹ To exclude this coupling process as an explanation for our satellite resonances we measured sample 3 in a tilted magnetic field. The CR and HER positions follow a $\cos\theta$ law up to $B_{\perp} \approx 4.5$ T. No splitting of the CR is observed, indicating that we are in the nonresonant limit, i.e., $\hbar\omega_c < E_{01}$. The sole influence of the coupling is that for $B_{\perp} \geq 4.5$ T the CR and HER energies are lower than predicted by the $\cos\theta$ law. The qualitatively similar tilt-angle dependence of the HER and the CR demonstrates that the HER is pinned to ω_c and that the HER is confinement related.

There may be evidence for inhomogeneity in our samples, as described above. Thus, for a nonparabolic and polar system like GaAs fluctuations in N_s of individual wells will correspond to different cyclotron frequencies. However, calculations show that these differences are small ($\lesssim 5 \text{ cm}^{-1}$). Shifts in ω_c which are comparable to ω_c (Fig. 2) cannot be related to inhomogeneity. Spin splitting is as well much too small to explain the satellite resonance positions. The presence of localized states can cause shifts in oscillator strength in cyclotron excitation and result as well in satellite resonances.¹⁰ However, the N_s dependence of our satellite resonances cannot be explained in this model which therefore can be excluded as a possible explanation.

We attribute the new satellite resonances to excitation of magnetic excitons since the number of observed resonances and their N_s and B dependences are consistent with theoretical predictions. In a system with weak interaction, i.e., $E_{\text{Coulomb}}/\hbar\omega_c \ll 1$, magnetic excitons can be classified as magnetoplasmons, spin waves, and coupled magnetoplasmon-spin modes.^{4,11} The magnetoplasmon modes associated with ω_c are the ones with the highest oscillator strength. Figure 3 shows calculated magnetoplasmon dispersions in single-layer approximation on the assumption of small interaction for the lowest integer filling factors $f=2\pi l^2 N_s$. Results are given for the densities of samples 1 and 3 with solid and dotted lines, respectively. Magnetoplasmon dispersions in spin-polarized state $f=1$ and fully occupied lowest Landau level $f=2$ with dashed and dash-dotted lines, respectively. Compared to the quasiclassical prediction, electron-electron interaction causes the magnetoplasmon frequencies to increase with q for $ql \gtrsim 2$, thus giving rise to additional divergencies in the density of states. In an experiment any excitation process which itself is not selective

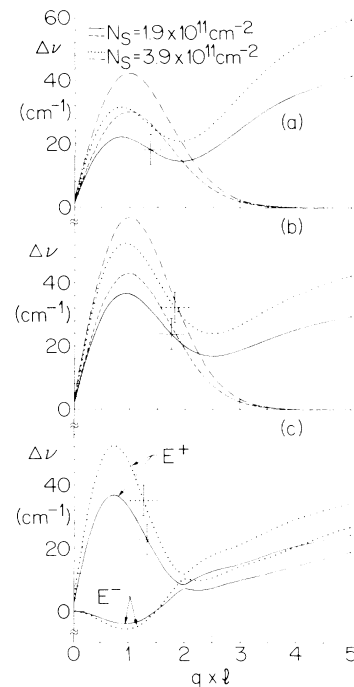


FIG. 3. Calculated shifts $\Delta\nu = \Delta\omega/2\pi c = \nu_{\text{ex}} - \nu_c$ of the magnetic exciton dispersions in single-layer approximation (Ref. 4) for samples 1 (solid line) and 3 (dotted line) and filling factors (a) $f=1$, (b) $f=2$, and (c) $f=3$. Dashed and dash-dotted curves present quasiclassical magnetoplasmon frequencies. The lines and bars indicate shifts ($\nu_{\text{HER}} - \nu_c$) and FWHM of the HER, respectively, and are positioned arbitrarily in the wave-vector regime $1 \leq ql \leq 2$.

in q , e.g., short-range scatterers,^{11,12} can induce resonant structures in the optical spectra with related energies. Scatterer-induced excitation is possible in our experiment since the satellites were found particularly pronounced in some MQW with low mobilities. However, light scattering via interface roughness, crystal imperfections, inhomogeneities in the well density, or impurities might as well contribute to the excitation process.¹³

If more than one Landau level is occupied and both spins are unequally present, two magnetoplasmon modes E^+ and E^- are predicted. Exemplarily this is shown in Fig. 3(c) for $f=3$. The E^- mode is a coupled magnetoplasmon-spin mode which does not exist for a noninteracting system ($E_{\text{Coulomb}}=0$). Therefore in the most general case the number of divergencies in the exciton density of states totals three, two with energies larger and one with energy smaller than ω_c , in contrast to only one for the noninteracting system. This agrees with our observation of three satellite resonances.

The shift of the HER to higher energies with N_s (Fig. 2) is consistent with the exciton theory. In Fig. 3, at fixed f , i.e., constant magnetic field strength, the exciton frequencies shift to higher energies with increasing N_s .

Since the extrema in the theoretical dispersions occur in a wave-vector range $1 \leq ql \leq 2$ we can restrict a quantitative comparison with the experiment to this regime. Experimental HER positions for samples 1 and 3 are marked with horizontal lines in the wave-vector regime of interest $1 \leq ql \leq 2$. In the high-field limit $f=1$ [Fig. 3(a)] there is good agreement between the experimental HER position and the extrema in the exciton dispersions. Because of the increasing interaction parameter $E_{\text{Coulomb}}/\hbar\omega_c$ with decreasing B , which ranges from 2.6 to 0.8 for the magnetic field regime from 1 to 12 T, no correspondence of the HER position with an extremum in the exciton dispersions is expected in the low-field limit $f \geq 2$. Stronger interaction enhances intermode coupling and reduces the exciton energies, although the form of the dispersion relations does not change qualitatively.⁵ Generally, the finite thickness of the space-charge layers and coupling of exciton modes of adjacent wells are important as well. However, for our MQW and $ql \geq 1$, influences of interwell coupling are expected to be small, because we are in the weak-coupling limit ($qd > 1$).

The B dependence of the HER (Fig. 2) is in qualitative agreement with the prediction. With decreasing filling factor ($f < 2$) the exciton energies decrease [Figs. 3(a) and 3(b)], which agrees with our observation that the HER approaches ω_c in the high-field limit. A decrease of the HER shift is also observed in the low-field limit. This behavior is due to an increase in Coulomb energy which leads to an increase of the excitonic mode coupling with decreasing magnetic field.⁵

The satellite with $\omega < \omega_c$ shows a qualitatively similar B dependence as the HER, whereas the satellite with $\omega > \omega_c$ approaches ω_c more rapidly with increasing B than does the HER and merges into the HER for low fields. The magnitude of the shift $|\omega - \omega_c|$ of those sa-

tellites increases as well with N_s which supports our interpretation that a plasmon oscillation is involved.

In conclusion new resonance structures are observed in the high-frequency magnetoconductivity of MQW on GaAs. Their number and dependence on N_s and B is consistent with predictions for the collective modes (magnetic excitons) of an interacting two-dimensional system in a magnetic field.

We gratefully acknowledge valuable discussions with C. Kallin and H. L. Störmer. We also wish to thank R. F. Kopf for assistance in molecular-beam-epitaxy growth and A. S. Jordan for his support.

^(a)Present address: Institut für Angewandte Physik, Universität Hamburg, Jungiusstrasse 11, 2000 Hamburg 36, West Germany.

¹K. W. Chiu and J. J. Quinn, Phys. Rev. B **9**, 4724 (1974).

²F. Stern, Phys. Rev. Lett. **18**, 546 (1967).

³Yu. A. Bychkov, S. V. Iordanskii, and G. M. Eliashberg, Pis'ma Zh. Eksp. Teor. Fiz. **33**, 152 (1981) [JETP Lett. **33**, 143 (1981)].

⁴C. Kallin and B. I. Halperin, Phys. Rev. B **30**, 5655 (1984).

⁵A. H. MacDonald, J. Phys. C **18**, 1003 (1985).

⁶J. C. Maan, M. Altarelli, H. Sigg, P. Wyder, L. L. Chang, and L. Esaki, Surf. Sci. **113**, 313 (1982).

⁷G. Abstreiter, J. P. Kotthaus, J. F. Koch, and G. Dorda, Phys. Rev. B **14**, 2480 (1976).

⁸Z. Schlesinger, S. J. Allen, J. C. M. Hwang, and P. M. Platzman, Phys. Rev. B **30**, 435 (1984).

⁹Z. Schlesinger, J. C. M. Hwang, and S. J. Allen, Phys. Rev. Lett. **50**, 2098 (1983).

¹⁰H. J. Mikeska and H. Schmidt, Z. Phys. B **20**, 43 (1975).

¹¹C. Kallin and B. I. Halperin, Phys. Rev. B **31**, 3635 (1985).

¹²C. S. Ting, S. C. Ying, and J. J. Quinn, Phys. Rev. Lett. **37**, 215 (1976).

¹³T. W. Nee, Phys. Rev. B **29**, 3225 (1984).